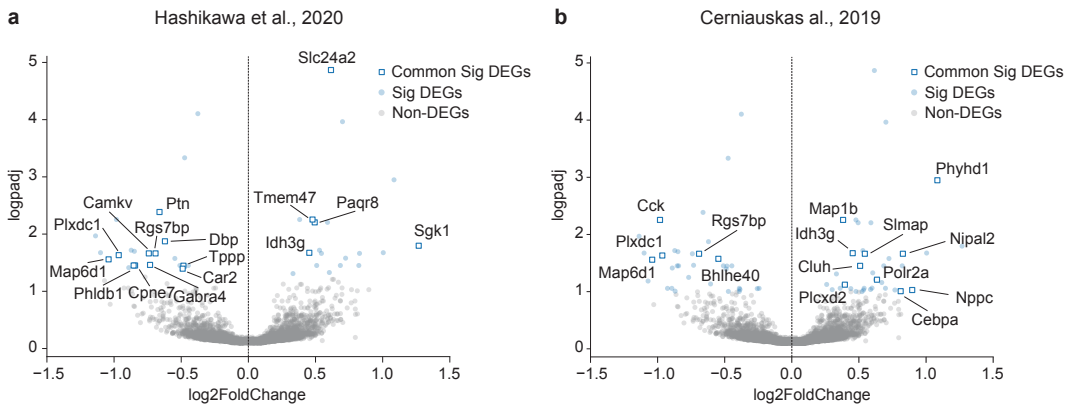


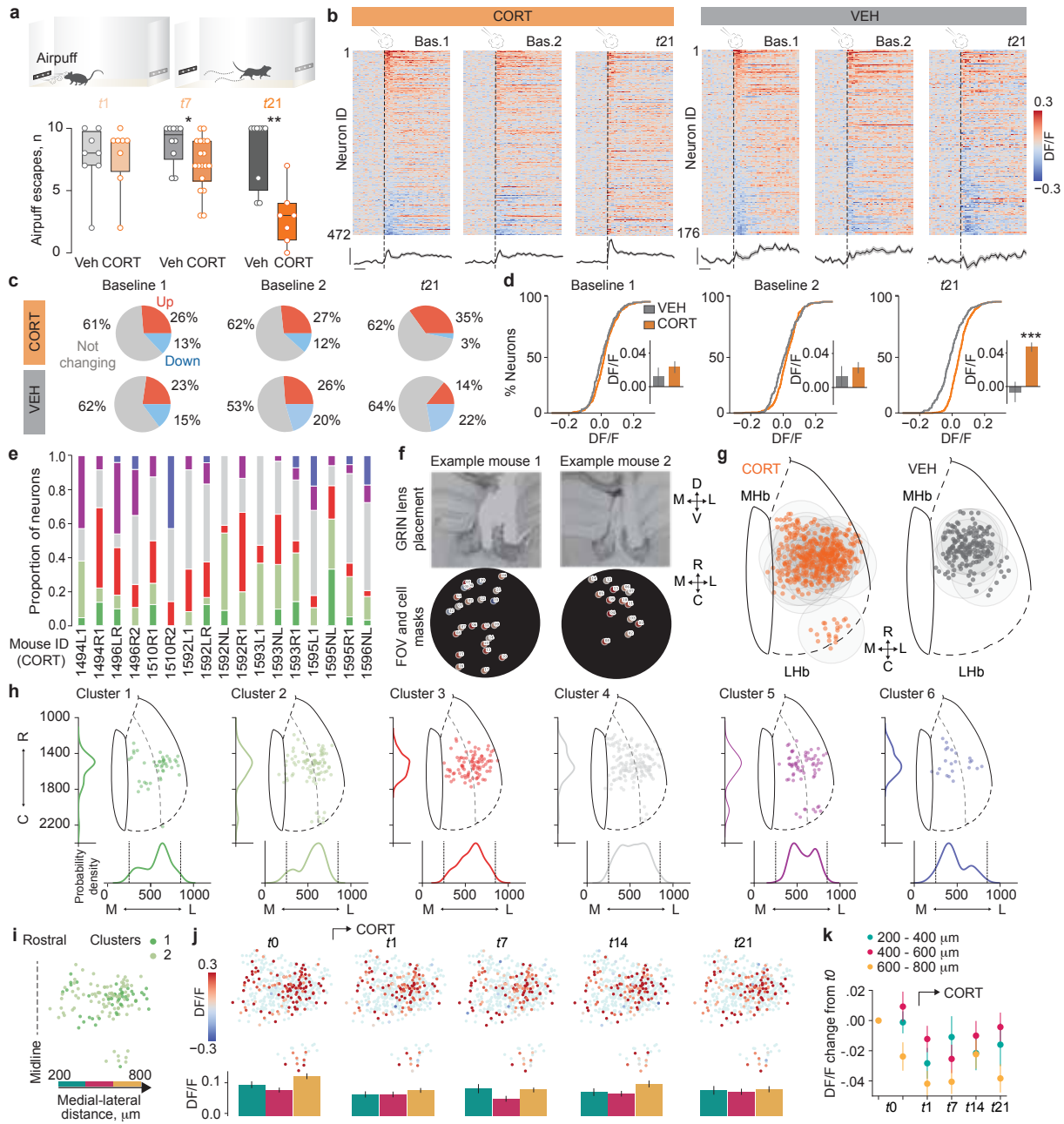
Molina et al., Extended Data Figure 1

**Extended Data Figure 1. Remodeling of a LHb molecular cartography in depression.** **a**, Violin plots showing distribution of UMI per barcode (top) and number of genes detected per barcode (bottom) in the habenular spots. **b, c**, UMAP visualization of habenula (Hb) spots color coded by normalized expression for MHb and LHb canonical gene markers, and markers for neurons, astrocytes, oligodendrocytes, microglia, endothelial cells and Oligodendrocyte Precursor Cells (OPC) based on Hashikawa et al., 2020 and Wallace et al., 2020 databases. **d**, PCA of LHb spots at baseline conditions color coded by normalized spatial coordinates (medio-lateral, ML; left, and dorso-ventral, DV; right). **e**, Regression analysis of the top five principal components (PCs) against spatial coordinates (ML, left, and DV, right), showing the contribution of spatial position to transcriptomic variance. **f**, Distribution of PC1 loading, dashed lines represent the 2 standard deviation thresholds used to classify genes as medially or laterally biased. **g**, Left, heatmap representation of z-scored expression of top 10 laterally (top) and medially (bottom) biased genes. Below, quantification of average expression of the genes classified as laterally biased, not biased or medially biased in (f). Right, expression gradient of two example genes laterally (top) and medially (bottom) biased, normalized within the LHb anatomical mask. **h**, Top, heatmap representation of z-scored expression; Bottom, spatial gradients within the LHb anatomical mask of the genes displayed in (g) using an independent spatial transcriptomics dataset (Han et al., 2025). **i**, Dot plot illustrating scaled expression levels (color) and percentage of expression (dot size) for the top 20 medially (left) and laterally (right) biased genes in (f) across cell types in the independent single-cell transcriptomics dataset<sup>23</sup>.



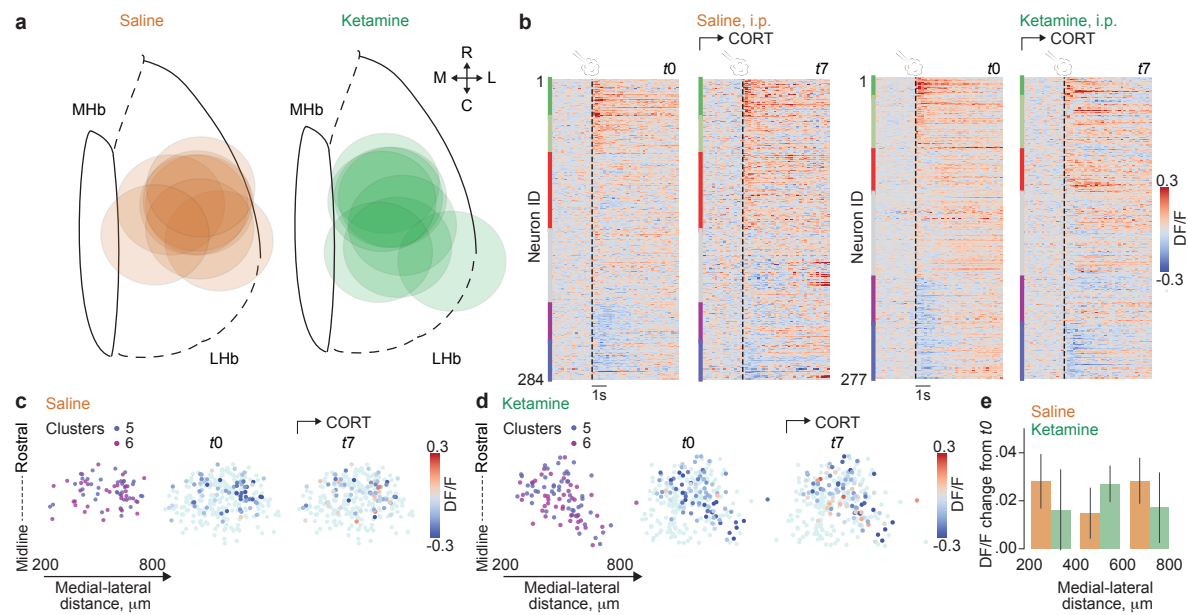
Molina et al., Extended Data Figure 2

**Extended Data Figure 2. Cross-validation of gene expression profile changes across different stress paradigms.** **a**, Volcano plot displaying DEGs induced by CORT treatment in the current dataset (see Fig. 1i). Blue data points denote genes significantly up- or down-regulated (Sig. DEGs) after CORT treatment and grey data points represent genes not significantly changed (non-DEGs). Annotated data points stem from re-analysis of published results. These annotated data points represent significant DEGs common between our current dataset and those obtained after footshock exposure in Hashikawa et al.<sup>23</sup> (*See Methods*). **b**, Same as (a), but annotated data points represent significant DEGs common between our current dataset and those obtained after chronic mild stress paradigm in Cerniauskas et al.<sup>21</sup> (*See Methods*).



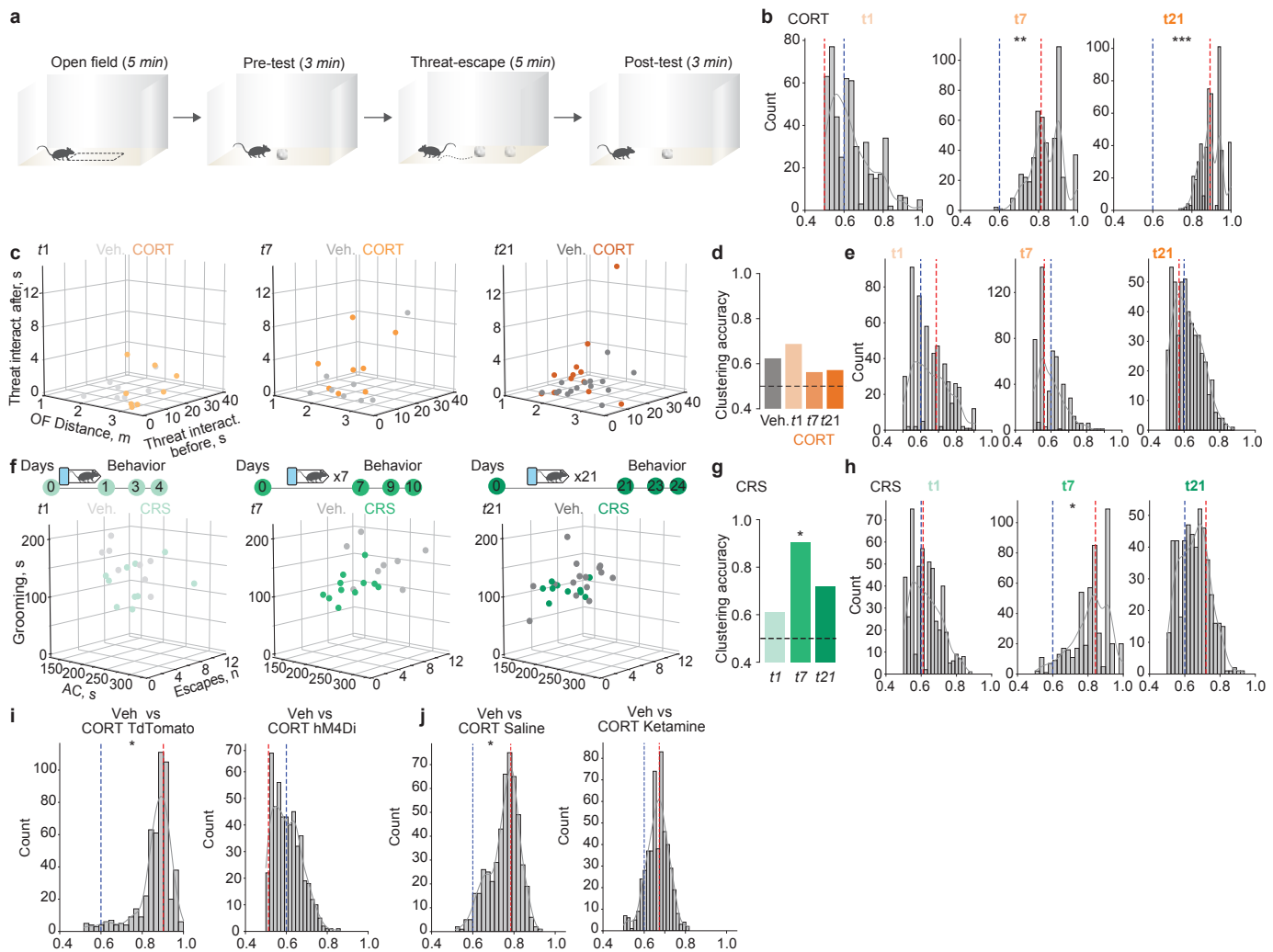
Molina et al., Extended Data Figure 3

**Extended Data Figure 3. Spatiotemporal dynamics of LHb neuronal activity across chronic CORT.** **a**, Schematic of the airpuff-driven escape paradigm. Independent cohorts of mice were treated with CORT ( $0.1 \text{ mg ml}^{-1}$ ) or vehicle (Veh) for 1 ( $n_{\text{Veh}} = 8$ ,  $n_{\text{CORT}} = 8$ ), 7 ( $n_{\text{Veh}} = 10$ ,  $n_{\text{CORT}} = 18$ ), or 21 days ( $n_{\text{Veh}} = 9$ ,  $n_{\text{CORT}} = 7$ ) and tested for airpuff-evoked escape behavior (Mann-Whitney test,  $U = 29.50$ ,  $P = 0.834$ ;  $U = 47$ ,  $*P = 0.035$ ;  $U = 4$ ,  $**P = 0.0014$ , for day 1, 7 and 21, respectively). Data represented as median  $\pm$  minimum-to-maximum whiskers. **b**, Heatmaps of individual neurons airpuff responses (dashed line) at baseline (Bas) 1, 2, and day 21 in CORT ( $n = 472$  cells, 17 mice) and vehicle mice ( $n = 176$  cells, 6 mice). Bottom, population average responses (scale bars,  $0.05 \text{ DF/F}$ , 1 s). **c**, Percentage of neurons displaying increased, unchanged, or reduced airpuff response at baseline 1, 2, and day 21 in CORT- and vehicle-treated mice. **d**, Distribution of airpuff responses at baseline 1, 2, and day 21 in vehicle- and CORT-treated mice (unpaired t-test,  $t_{646} = 1.8$ ,  $P = 0.07$ ;  $t_{646} = 1.67$ ,  $P = 0.09$ ;  $t_{646} = 9.22$   $***P < 0.001$ , respectively). **e**, Histological sections of GRIN lens placement and corresponding FOVs with individual neurons masks. **f**, Anatomical reconstruction of GRIN lens position and individual neurons masks projected onto LHb horizontal plane in CORT and vehicle mice. **g**, Distribution of neurons across clusters in individual CORT-treated mice. **h**, Anatomical reconstruction of neurons putative location in LHb horizontal plane for each cluster in CORT condition and quantification of the probability density along medio-lateral and rostro-caudal axes. **i**, Spatial projection onto horizontal plane of cluster 1-2 neurons in CORT mice. **j**, Spatial projection of all neurons (light blue) with superimposed color-coded airpuff responses of clusters 1-2 across recording sessions. Below, average airpuff responses per  $200 \mu\text{m}$  medio-lateral bin. **k**, Average airpuff-induced DF/F change from  $t0$  across medio-lateral bins and sessions (Two-way RM ANOVA, Interaction,  $F_{10,665} = 1.69$ ,  $P = 0.079$ ). Data represented as mean  $\pm$  s.e.m.



Molina et al., Extended Data Figure 4

**Extended Data Figure 4. Antidepressant-purposed ketamine restores CORT-mediated LHb remodeling.** **a**, Anatomical reconstruction of GRIN lens position into the horizontal plane of LHb in saline- and ketamine-treated mice. **b**, Heatmaps of individual neurons average DF/F responses to airpuff (dashed line) at  $t0$  (average baseline 1 and 2) and day 7 of CORT treatment in mice administered intraperitoneally with either saline ( $n = 284$  cells, 8 mice) or ketamine ( $n = 277$  cells, 8 mice). Neurons were sorted according to cluster identity. **c**, Spatial projection of neurons from clusters 5 and 6 onto the horizontal plane (left) and of all recorded neurons with superimposed color-coded airpuff response in neurons from clusters 5 to 6 at  $t0$  and day 7 of recording in saline-treated mice. **d**, Same as (c) in ketamine-treated mice. **e**, Average airpuff-induced DF/F change from baseline across bins at day 7 in saline- and ketamine-treated mice (Two-way ANOVA, Treatment,  $F_{1,158} = 0.004$ ,  $P = 0.95$ ). Data are mean  $\pm$  s.e.m.



Molina et al., Extended Data Figure 5

**Extended Data Figure 5. Time-resolved emergence of behavioral signatures of depression.** **a**, Schematic diagram of open field and threat-escape task. **b**, Statistical significance was computed using bootstrap between the different experimental groups (Veh and CORT at day 1,  $P = 0.335$ , left; day 7,  $P = 0.005$ , middle, and day 21,  $P = 0.004$ , right). **c**, 3-dimensional plots showing individual behavioral scores – distance travelled, and time interacting with the threat before and after the threat-escape task – from vehicle- and CORT-treated mice after 1 (left), 7 (middle) or 21 (right) days of treatment. **d**, Clustering accuracy from k-means classification using behavioral scores in veh group vs remaining veh groups (grey) and CORT groups vs their respective time-match veh groups (orange) and **e**, Statistical significance determined by bootstrap. **f**, Top, schematics of chronic restraint stress (CRS) and bottom, 3-dimensional plots showing individual behavioral scores – number of threat-evoked anticipatory escapes, active coping (AC, s) in the TST and grooming time during the apathy-like paradigm – from vehicle controls and CRS-exposed mice after 1 (left,  $n_{\text{Veh}}=8$  and  $n_{\text{CRS}}=10$ ), 7 (middle,  $n_{\text{Veh}}=8$  and  $n_{\text{CRS}}=11$ ) or 21 (right,  $n_{\text{Veh}}=15$  and  $n_{\text{CRS}}=10$ ) days. **g**, Clustering accuracy from k-means classification using behavioral scores of each CRS group versus their respective time-matched vehicle control group. **h**, Bootstrap of clustering accuracy for CRS groups versus their respective time-matched vehicle group ( $p=0.4$ ,  $P = 0.04$  and  $P = 0.26$  after 1, 7, or 21 days of CRS, respectively). **i**, Bootstrap of clustering accuracy for either TdTomato-CORT or hM4Di-CORT groups vs all vehicle-treated mice ( $P = 0.026$  and  $P = 0.494$  respectively). **j**, Bootstrap of clustering accuracy for either Saline-CORT or Ketamine-CORT vs all vehicle-treated mice ( $P = 0.026$  and  $P = 0.104$ , respectively).

**Extended Data Table 1. Supporting information for gene ontology enrichment analysis for Fig. 1k.** Data table showing detailed results from performing gene ontology (GO) enrichment analysis for Biological Processes on the differentially expressed genes (DEG) in the lateral LHb in Fig. 1k.

**Extended Data Table 2. Detailed statistical analysis.** Data table shows a detailed summary of statistical tests for each figure panel when appropriate.